



HAL
open science

Constrained Optimal Control Problem Applied to Vaccination for COVID-19 Epidemic

Hani Abidi, Rim Amami, Chiraz Trabelsi

► **To cite this version:**

Hani Abidi, Rim Amami, Chiraz Trabelsi. Constrained Optimal Control Problem Applied to Vaccination for COVID-19 Epidemic. 2022. hal-03476454v2

HAL Id: hal-03476454

<https://hal.science/hal-03476454v2>

Preprint submitted on 11 Mar 2022 (v2), last revised 17 Nov 2023 (v3)

HAL is a multi-disciplinary open access archive for the deposit and dissemination of scientific research documents, whether they are published or not. The documents may come from teaching and research institutions in France or abroad, or from public or private research centers.

L'archive ouverte pluridisciplinaire **HAL**, est destinée au dépôt et à la diffusion de documents scientifiques de niveau recherche, publiés ou non, émanant des établissements d'enseignement et de recherche français ou étrangers, des laboratoires publics ou privés.

Constrained Optimal Control Problem Applied to Vaccination for COVID-19 Epidemic

Hani Abidi¹, Rim Amami², Chiraz Trabelsi³

11 mars 2022

Résumé

COVID-19 remains a major threat to the world since its emergence in December 2019, especially the lack of identification of a specific treatment, as scientific researchers continue to seek a better understanding of the epidemiological cycle and dynamics of the virus. Mathematical modeling of the COVID-19 disease can provide better insight into the complex dynamics of the virus and define preventive measures that can be used to contain the spread of the disease. In this research article, we propose a model describes the epidemic dynamics of Covid-19 in a population after vaccine deployment, is an extension of the standard SEAIR model incorporating temporary protection vaccine compartment. An optimal control problem is formulated with the aim of minimizing the number of infected individuals while considering intervention costs and the constraints of the total and maximum daily vaccine administration. We use the penalty method to approximate this constrained optimization problem and derive an optimality system that characterizes the optimal control. Finally, we carry out numerical simulations using reported data on COVID-19 infections and vaccination in France and in Tunisia, compare these two countries in the face of the pandemic.

Keywords : Covid-19 Epidemic, Control constraints, Mathematical modeling of COVID-19, Maximum Principle, Optimal control problem, Ordinary differential equations, Vaccination.
MSC Classification : 34H05, 49J15.

1 Introduction

Appeared in December 2019 in Wuhan, mainland China, COVID-19 very quickly turned out to be a serious health problem around the world, with catastrophic consequences for the evolution of humankind. Our modern world has never been confronted. This disease of such magnitude. All statistics data about coronavirus COVID-19 comes from World Health Organization, Johns Hopkins CSSE and worldometers. Charts includes number of infected, deaths and recovered people. Until December 2021, estimate around 270 million people have been infected, of which there are more than 5.32 million deaths.

There is now no medicine or specific treatment for the COVID-19, most countries had been relying on non-pharmaceutical interventions, such as wearing of face masks, washing hands and take care of personal hygiene, physical distancing and even more partial or total lockdown in order to curtail the spread of the disease. However, these measures have been not an effective protection to mitigate the pandemic globally. To bring this pandemic to an end, a large share of the world needs to be immune to the virus. The safest way to achieve this is with a vaccine. Within less than 12 months after the beginning of the COVID-19 pandemic, several research teams rose to the challenge and developed vaccines that protect from SARS-CoV-2. Until December 2021,

¹abidiheni@gmail.com, Esprit School of Business, Tunisia.

²rabamami@iau.edu.sa, Department of Basic Sciences, Deanship of Preparatory Year and Supporting Studies, Imam Abdulrahman Bin Faisal University, P.O. Box 1982, Dammam 34212, Saudi Arabia.

³chiraz.trabelsi@univ-mayotte.fr, Centre Universitaire de Mayotte, 8 rue de l'université BP53, 97660 Dembeni, Mayotte, IMAG Montpellier, France.

8.45 billion doses have been administered globally, and 56% of the world population has received at least one dose of a COVID-19 vaccine.

The study of the novel coronavirus has relatively attracted some importance in mathematical epidemiology due to its seriousness and the way it spreads worldwide. For instance, several models have been proposed to provide insight into the effect that inoculation of a certain portion of the population will have on the dynamics of the COVID-19 pandemic. The motivation of this study is derived from the work [3], who adopt a more modelling approach based on optimal control theory to determine the best strategy to implement until vaccine deployment. Therefore, in the present study, we incorporate the vaccination component to the model in [3], to derive an extended SEAIR model to examine the effectiveness of the COVID-19 jabs which are currently being deployed to many countries to help combat the raging pandemic situation.

Since the identification of the novel virus SRAS-COV-2 and the spread of the global COVID-19 pandemic, several authors have been attracted by this area and have investigated the epidemic model of COVID-19, such as [5] which implemented some epidemic models for Cholera and COVID-19 in Yemen through mathematical analysis. The authors propose a new dynamic mathematical model framework governed by a system of differential equations that integrates both COVID-19 and cholera outbreaks.

Another new study is that by [2, 13] which the authors use a stochastic approach to study and simulate the COVID-19 model.

The importance of the isolation strategy was emphasized in [2] to reduce the infection of COVID-19. The authors prove the existence and uniqueness of a global positive solution for a COVID-19 stochastic model with isolation strategy. The white noise and the Levy jump perturbations are incorporated in all compartments of the suggested model. Some numerical simulations are presented to illustrate the theoretical results.

For a stochastic COVID-19 model with jump-diffusion, the authors prove in [13] the existence and uniqueness of the global positive solution. They also investigate some conditions for the extinction and persistence of the disease. The main contribution of this paper is to conclude that the stochastic model is more realistic than the deterministic one.

The authors in [10] apply optimal control theory to determine optimal strategies for the implementation of non-pharmaceutical interventions to control COVID-19. The studied model was calibrated to data from the USA and focused the analysis on optimal controls from May 2020 through December 2021.

Other authors have focused on the problem of optimal control theory to study and extend various epidemiological models. Among others [4] where the optimal control theory is applied to suggest the most effective mitigation strategy to minimize the number of individuals who become infected in the course of an infection while efficiently balancing vaccination and treatment applied to the models. The SIR model analysis is presented here including the proof of uniqueness and existence of the optimal control solutions.

In the same area, the authors in [3] use optimal control theory to explore the best strategy to implement while waiting for the vaccine. The main contribution of this paper is to find a solution minimizing deaths and costs due to the implementation of the control strategy itself.

The authors in [9] propose and analyse an extended SEIARD model with vaccination to examine the effectiveness of the COVID-19 jabs which are currently being deployed to many countries to help combat the raging pandemic situation. Some numerical simulations are achieved using reported data on COVID-19 infections and vaccination in Mexico.

This paper is composed of four sections. We first present in Section 2, the structure of our epidemiological model, precisely we present the equations and assumptions of the extended SEAIR model with vaccination. In Section 3 we introduce the objective function and a reformulation of the optimal control problem to minimize the incidence satisfying the constraints of the total and maximum daily vaccine administration and we derive the optimality condition. We use the penalty method to approximate this constrained optimization problem and derive an optimality system that characterizes the optimal control. In Section 4, we carry out numerical simulations

using reported data on COVID-19 infections and vaccination in France and in Tunisia, compare these two countries in the face of the pandemic, and conclude with a summary.

2 The Model

The model describes the epidemic dynamics of Covid-19 in a population after vaccine deployment, is an extension of the standard SEAIR model incorporating temporary protection vaccine compartment to the model [3], regardless of the disease severity whether mild or severe infections. To derive the mathematical model, first we subdivide our population into two subpopulation, the unvaccinated population and vaccinated population (individuals who have received one, two or three doses of the vaccine). The model classifies individuals into principle key compartments of :

- Susceptible (S).
- Latent (E) : infected but asymptomatic and not infectious.
- Asymptomatic infectious (A).
- Symptomatic infectious (I).
- Immune (R) or Death (D).
- Temporary protection vaccine (VP) which has two issues : Vaccine susceptible (VS) or vaccine immune (VR).

Figure 1 illustrates the different compartments for the model SEAIR with vaccination.

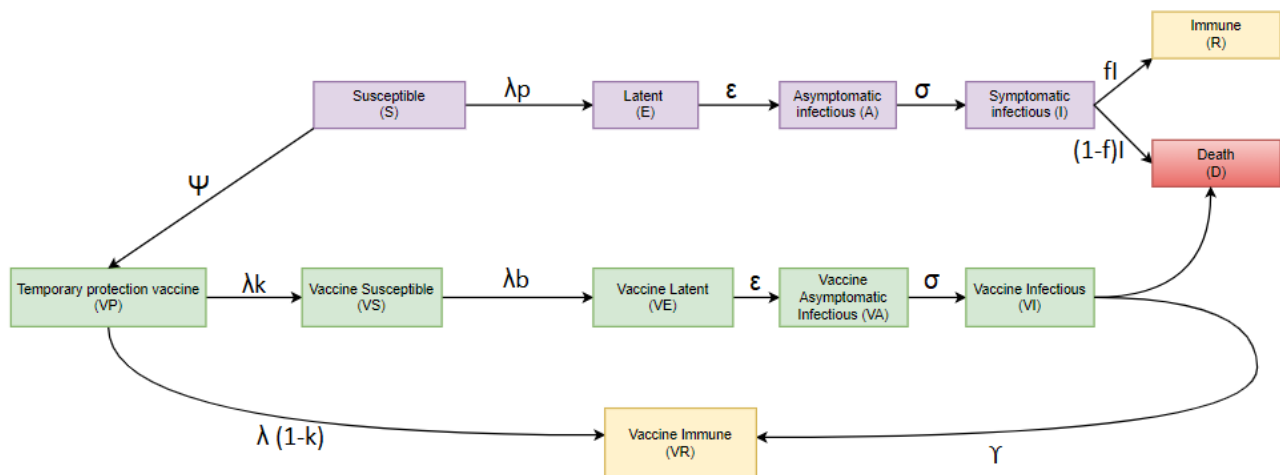


FIGURE 1 – flow diagram for the SEAIR model with vaccination

The total population size at a given time t is given by

$$N(t) = S(t) + E(t) + A(t) + I(t) + R(t) + V(t).$$

We denote by c the control effort, and β_A , β_I are asymptomatic and symptomatic transmission rate respectively and for simplicity, we define the force of infection without indicating the time dependency by $\lambda = (1 - c)(\beta_A A + \beta_I I)$. A proportion p of exposed individuals (λS) move to the asymptomatic infection class at a rate ϵ , while the remainder susceptible individuals are vaccinated with vaccine efficacy ψ , are temporary protected. A proportion k of temporary protected individuals λVP move to vaccine susceptible while the remainder are vaccine immune

(VR), and a proportion b of exposed vaccine individuals (λVS) move to the asymptotic infection at rate ϵ . In the both case asymptomatic infectious, unvaccinated individuals or vaccinated individuals, become symptomatic at rate σ , and recover at rates f and γ respectively.

The principal parameters used throughout this paper and their interpretation are as follows :

- I^* : the total number of infected hosts the health care system, or simply the healthcare capacity.
- μ : natural hospitality rate with hospital saturation.
- mortality rate for all population $\mu[I] = \begin{cases} 0 & \text{if } I < I^* \\ \mu & \text{if } I \geq I^* \end{cases}$
- α : bound disease induced mortality rate.
- Mortality rate $\alpha[I] = \begin{cases} \alpha_{min} & \text{if } I < I^* \\ \alpha_{max} & \text{if } I \geq I^* \end{cases}$
- $c \in (0, 1)$: control effort. The time dependent control function $c(t)$ measures the rate at which susceptible individuals are vaccinated.
- force infection : $\lambda = (1 - c)(\beta_A A + \beta_I I)$ where $\begin{cases} \beta_I = & \text{symptomatic transmission rate} \\ \beta_A = & \text{asymptomatic transmission rate} \end{cases}$
- ψ : susceptible individuals are vaccinated with vaccine efficacy ψ .
- k : loss of vaccine protection.
- p : proportion of infections unvaccinated individuals.
- b : proportion of infections vaccinated individuals.
- ϵ : waiting rate to viral shedding.
- σ : waiting rate to symptom onset.
- f : recovery rate from infections unvaccinated individuals.
- γ : recovery rate from infections vaccinated individuals.
- $(1 - f)$: death rate of infectious unvaccinated individuals
- $(1 - \gamma)$: death rate of infectious vaccinated individuals with symptoms

Hence, our model is described by the following system of ODEs : (assume $x'(t) = \frac{dx(t)}{dt}$)

$$\begin{aligned}
(1) \quad S'(t) &= -\lambda p S(t) - \psi c(t) S(t) - \mu[I] S(t) \\
(2) \quad E'(t) &= p \lambda S(t) - (\epsilon + \mu[I]) E(t) \\
(3) \quad A'(t) &= \epsilon E(t) - \sigma A(t) - \mu[I] A(t) \\
(4) \quad I'(t) &= \sigma A(t) - (f + \mu[I]) I(t) \\
(5) \quad R'(t) &= f I(t) - \mu[I] R(t) + \psi c(t) S(t) \\
(6) \quad VP'(t) &= \psi S(t) - k \lambda \mu[I] VP(t) \\
(7) \quad VS'(t) &= \psi S(t) + k \lambda VP(t) - (b \lambda + \mu[I]) VS(t) \\
(8) \quad VE'(t) &= b \lambda VS(t) - (\epsilon + \mu[I]) VE(t) \\
(9) \quad VA'(t) &= \epsilon VE(t) - (\sigma + \mu[I]) VA(t) \\
(10) \quad VI'(t) &= \sigma VA(t) - (\gamma + \mu[I]) VI(t) \\
(11) \quad VR'(t) &= \gamma VI(t) - \mu[I] VR(t) + (1 - k) \lambda VP(t) \\
(12) \quad D'(t) &= \alpha[I] I(t) + \mu[I] N - \gamma VR(t) + (1 - \gamma) VI(t)
\end{aligned}$$

with the following initial conditions

$$\begin{aligned}
S(0) &= S_0 = N_0 - I_0 \\
(13) \quad E(0) &= A(0) = R(0) = VS(0) = VE(0) = VA(0) = VI(0) = VP(0) = VR(0) = 0 \\
D(0) &= 0.
\end{aligned}$$

Figure 1 shows a flow diagram for model (1) and points out the different parameters used.

Remark 2.1 Equations (6), (7), (8), (9), (10), and (11) can be replaced by the following global equation :

$$(14) \quad V'(t) = \psi S(t) - k \lambda V(t) - (1 - f) I(t) + \gamma V(t).$$

In summary, the nonlinear system of ODEs describing the COVID-19 dynamics under the initial conditions (26) can be written as follows :

$$(15) \quad \begin{cases} S'(t) = & -\lambda p S(t) - \psi c(t) S(t) - \mu [I] S(t) \\ E'(t) = & p \lambda S(t) - (\epsilon + \mu [I]) E(t) \\ A'(t) = & \epsilon E(t) - \sigma A(t) - \mu [I] A(t) \\ I'(t) = & \sigma A(t) - (f + \mu [I]) I(t) \\ R'(t) = & f I(t) - \mu [I] R(t) + \psi c(t) S(t) \\ V'(t) = & \psi S(t) - k \lambda V(t) - (1 - f) I(t) + \gamma V(t) \\ D'(t) = & \alpha [I] I(t) + \mu [I] N - \gamma V R(t) + (1 - \gamma) V I(t). \end{cases}$$

3 Objective function

The strategy consists to minimize the number of people infected after vaccination. The control scheme is optimal if it minimizes the following objective function

$$(16) \quad J(c) = \int_0^T [PI(t) + Bc^2(t)] dt.$$

The first integral corresponds to the total number of infected individuals by the Covid-19 Epidemic. The second one represents the total cost associated with the implementation of the control measure. It's a quadratic expression to find a known solution (for more details see [8]).

B is a coefficient allowing to weight the "cost" associated to the control implementation c .

The goal of this paper is to find a function c^* such that

$$J(c^*) = \min J(c).$$

To find the optimal control $c^*(t)$, that minimizes $J(c)$, we follow standard results from optimal control theory applied to systems of ordinary differential equations. Usually, when the world has faced its most dangerous pandemic, the vaccination coverage (proportion of vaccinated people in a population at a given time) and the maximum daily vaccine administration are limited, therefore our model integrates these realistic constraints using state variable inequality constraints. This can be stated as follows :

$$(17) \quad \begin{cases} 0 & \leq c(t) \leq 1 \\ c(t)S(t) & \leq c_{max} \\ \int_0^T c(t)S(t)dt & \leq c_{total} \end{cases}$$

where c_{max} is the maximum daily vaccination and c_{total} is the vaccine coverage.

Our goal is to minimize the number of infected individuals using a limited total vaccination which implies to minimize $J(c)$.

The main tool that can be used is the Pontryagin's Maximum Principle which is helpful to prove the existence of an optimal solution of the constrained minimization problem.

Let us introduce the following auxiliary state variable

$$z(t) = \int_0^t c(s)S(s)ds.$$

Then, we get

$$(18) \quad \begin{cases} z'(t) = & c(t)S(t) \\ z(0) = & 0 \\ z(T) \leq & c_{total} \end{cases}$$

So the constrained minimization problem associated to (17) and (18) becomes :

$$(19) \quad \begin{cases} z'(t) & = c(t)S(t) \\ z(0) & = 0 \\ z(T) & \leq c_{total} \\ 0 & \leq c(t) \leq 1 \\ c(t)S(t) & \leq c_{max} \end{cases}$$

Using the monotonically increasing property of $z(t)$, we get

$$z(T) \leq c_{total} \quad \text{is equivalent to} \quad z(t) \leq c_{total}.$$

Theorem 3.1 *There exists an optimal solution to the problem (19).*

The existence of an optimal solution of the constrained minimization problem (19) is proved using the following Filippov-Cesari existence theorem ([1, 11]) :

Theorem 3.2 [1] *Let $x(t) = (x_1(t), \dots, x_n(t)) \in \mathbb{R}^n$ be a state vector and $u(t) = (u_1(t), \dots, u_r(t)) \in \mathbb{R}^r$ be a control vector associated to the following optimal control problem*

$$(20) \quad \min \int_{t_0}^{t_1} F(x(t), u(t), t) dt.$$

with

$$(21) \quad \dot{x} = f(x(t), u(t), t), \quad x(t_0) = x^0,$$

with the terminal conditions

$$(22) \quad \begin{aligned} x_i(t_1) &\geq x_i^1, & i = 1, \dots, m \\ x_i(t_1) &\text{ free}, & i = m+1, \dots, n. \end{aligned}$$

and for $u(t) \in U$, with U is a fixed set in \mathbb{R}^r we have the following constraints

$$(23) \quad g(x(t), u(t), t) \geq 0.$$

Assume that there exists an admissible pair $(x(t), u(t))$ and

1. U is closed.
2. $N(x, t) = \{y = (y, y_{n+1}) : y = f(x, u, t), y_{n+1} \geq F(x, u, t), g(x, u, t) \geq 0, u \in U\}$ is convex for all $(x, t) \in \mathbb{R}_n \times [t_0, t_1]$.
3. There exists a number $\theta > 0$ such that $\|x(t)\| < \theta$ for all admissible pairs $(x(t), u(t))$, and all $t \in [t_0, t_1]$.
4. There exists an open ball $B(0, \gamma) \subset \mathbb{R}^r$ which contains the set $\Omega(x, t) = \{u \in U : g(x, u, t) \geq 0\}$ for all $x \in B(0, \theta)$.

Then there exists an optimal pair $(x^*(t), u^*(t))$ to the problem (21),(22),(23) with $u^*(t)$ measurable.

Proof of Theorem 3.1. First remember the nonlinear system of ODEs (15) describing the COVID-19 dynamic :

$$\begin{cases} S'(t) & = -\lambda p S(t) - \psi c(t) S(t) - \mu [I] S(t) \\ E'(t) & = p \lambda S(t) - (\epsilon + \mu [I]) E(t) \\ A'(t) & = \epsilon E(t) - \sigma A(t) - \mu [I] A(t) \\ I'(t) & = \sigma A(t) - (f + \mu [I]) I(t) \\ R'(t) & = f I(t) - \mu [I] R(t) + \psi c(t) S(t) \\ V'(t) & = \psi S(t) - k \lambda V(t) - (1 - f) I(t) + \gamma V(t). \end{cases}$$

We assume that $x(t) = (S(t), E(t), A(t), I(t), R(t), V(t), z(t))^T$, $u(t) = c(t)$ and $F(x(t), u(t), t) = Px_3(t) + Bu^2(t)$. Then, we get

$$(24) \quad f(x(t), u(t), t) = \begin{bmatrix} -\lambda pS(t) - \psi c(t)S(t) - \mu[I]S(t) \\ p\lambda S(t) - (\epsilon + \mu[I])E(t) \\ \epsilon E(t) - \sigma A(t) - \mu[I]A(t) \\ \sigma A(t) - (f + \mu[I])I(t) \\ fI(t) - \mu[I]R(t) + \psi c(t)S(t) \\ \psi S(t) - k\lambda V(t) - (1-f)I(t) + \gamma V(t) \\ c(t)S(t) \end{bmatrix}$$

and $g(x(t), u(t), t) = c_{max} - u(t)x_1(t)$. Note that F, f and g are of class C^1 and f is bounded. Then, there exists a solution for the system (15) which guarantees an admissible pair $(x(t), u(t))$. By using that the control function c is verifying $0 < c(t) < 1$, and for that the control set $U = [0, 1]$ is compact, conditions of Filippov-Cesari existence theorem are verified.

The control set U is convex, so $f(x, u, t) = \alpha(x, t) + \beta(x, t)u$, $F(x, ., t)$ and $g(x(t), ., t)$ are convex on U .

The function f is expressed as a linear function of the control variable with coefficients dependent on the state variables and time in (24), and F and g are convex on U . Then $N(x, t)$ is convex, which is Condition 2 of Theorem 3.2.

Condition 3 follows from the boundedness of solutions to the system (15) for the finite time interval. ■

3.1 Penalty Method

A classic approach to handle the constrained optimal control problems is to use the penalty function method, which reformulates the original constrained problem into an unconstrained minimization problem that is solved by using a dynamic minimization algorithm. A penalty function of the constrained minimization problem (19) is

$$J_p(c) = \int_0^T \left[PI(t) + Bc^2(t) + \mu_1(c(t)S(t) - c_{max})^2 H_1(c(t)S(t) - c_{max}) \right. \\ \left. + \mu_2(z(t) - c_{total})^2 H_2(z(t) - c_{total}) \right] dt$$

where P, B are constants, μ_1, μ_2 are penalty parameters, $H_1(c(t)S(t) - c_{max}) = \begin{cases} 0 & \text{if } c(t)S(t) \leq c_{max} \\ 1 & \text{if } c(t)S(t) > c_{max} \end{cases}$

and $H_2(z(t) - c_{total}) = \begin{cases} 0 & \text{if } c(t)S(t) \leq c_{total} \\ 1 & \text{if } c(t)S(t) > c_{total} \end{cases}$

Then, to minimize the solution of constrained optimization problem (19), we should minimize $J_p(c)$, mainly to find the control c^* so as to minimise $J_p(c)$ subject to the nonlinear system of ODEs (15)

$$(25) \quad z'(t) = c(t)S(t), \quad z(0) = 0, \quad 0 \leq c(t) \leq 1.$$

Pontryagin's Maximum Principle is used to derive the optimality system which provides necessary conditions of the optimal solutions of (25).

In this case, we can write the augmented Hamiltonian for the constraints control as follow ,

$$\begin{aligned}
L(x, u, \lambda) = & PI(t) + Bc^2(t) + \mu_1(c(t)S(t) - c_{max})^2 H_1(c(t)S(t) - c_{max}) \\
& + \mu_2(z(t) - c_{total})^2 H_2(z(t) - c_{total}) + \lambda_1(t)(-\lambda p S(t) - \psi c(t)S(t) - \mu[I]S(t)) \\
& + \lambda_2(t)(p\lambda S(t) - (\epsilon + \mu[I])E(t)) + \lambda_3(t)(\epsilon E(t) - (\sigma + \mu[I])A(t)) \\
& + \lambda_4(t)(\sigma A(t) - (f + \mu[I])I(t)) + \lambda_5(t)(fI(t) - \mu[I]R(t) + \psi c(t)S(t)) \\
& + \lambda_6(t)(\psi S(t) - k\lambda V(t) - (1 - f)I(t) + \gamma V(t)) + \lambda_7(t)c(t)S(t) \\
& - \omega_1(t)c(t) - \omega_2(t)(1 - c(t)).
\end{aligned}$$

and we recall $\lambda = (1 - c)(\beta_A A + \beta_I I)$, here we use ω_1 et ω_2 as a penalty multipliers such that $\omega_1(t)$ and $\omega_2(t) \geq 0$ and

$$\omega_1(t)c(t) = \omega_2(t)(1 - c(t)) = 0, \quad \text{at } c = c^*.$$

On differentiating the augmented Lagrangian L with respect to state variables and setting the result to zero, we get the following adjoint system

$$\begin{aligned}
\lambda'_1 = -\frac{\partial L}{\partial S} &= -2\mu_1 c(t)(c(t)S(t) - c_{max})^2 H_1(c(t)S(t) - c_{max}) + \lambda p(\lambda_1(t) - \lambda_2(t)) + \lambda_1(t)\mu[I] \\
&\quad c(t)(\psi\lambda_1(t) - \psi\lambda_5(t) - \lambda_7(t)) - \lambda_6(t)\psi \\
\lambda'_2 = -\frac{\partial L}{\partial E} &= \epsilon(\lambda_2(t) - \lambda_3(t)) + \lambda_2(t)\mu[I] \\
\lambda'_3 = -\frac{\partial L}{\partial A} &= p(1 - c)\beta_A(\lambda_1(t) - \lambda_2(t))S(t) + \sigma(\lambda_3(t) - \lambda_4(t)) \\
&\quad + \mu[I]\lambda_3(t) + k(1 - c)\beta_A\lambda_6(t)V(t) \\
\lambda'_4 = -\frac{\partial L}{\partial I} &= P + p(1 - c)\beta_I(\lambda_1(t) - \lambda_2(t))S(t) + f(\lambda_4(t) - \lambda_5(t)) \\
&\quad + \mu[I]\lambda_4(t) + \lambda_6(t)(k(1 - c)\beta_I V(t) + (1 - f)) \\
\lambda'_5 = -\frac{\partial L}{\partial R} &= \lambda_5(t)\mu[I] \\
\lambda'_6 = -\frac{\partial L}{\partial V} &= \lambda_6(k\lambda - \gamma) \\
\lambda'_7 = -\frac{\partial L}{\partial z} &= -2\mu_2(z(t) - c_{total})H_2(z(t) - c_{total}).
\end{aligned}$$

with the transversality conditions $\lambda_i(T) = 0$, for $i = \{1, \dots, 7\}$. now, we differentiate the augmented Lagrangian L with respect to c :

$$\frac{\partial L}{\partial c} = 2Bc(t) + 2\mu_1(c(t)S(t) - c_{max})S(t)H_1(c(t)S(t) - c_{max}) - (\psi\lambda_1(t) - \psi\lambda_5(t) - \lambda_7(t))S(t) - \omega_1(t) + \omega_2(t) = 0.$$

To sum up, we find the optimal control by solving the state system with initial conditions and adjoint equations, we obtain

$$c^* = \min \left\{ 1, \max \left\{ 0, \frac{2\mu_1 c_{max} S(t) H_1(c(t)S(t) - c_{max}) + (\psi\lambda_1(t) - \psi\lambda_5(t) - \lambda_7(t))S(t) - \omega_1(t) - \omega_2(t)}{2(B + \mu_1 S^2(t) H_1(c(t)S(t) - c_{max}))} \right\} \right\}$$

4 Numerical simulations and discussion

Based on the real data collected from two countries Tunisia and France (december 15, 2020 to July 31 2021), this section will illustrate the mathematical results presented above by different numerical simulations.

In this section, we will simulate the solutions of the SEAIR model (1) to estimate the impact of

the vaccination program.

In Tunisia, massive vaccination started in March 2021 to combat the COVID-19 pandemic. Tunisia has only acquired two-dose vaccines. It recently granted a Marketing Authorization to Johnson and Johnson vaccine, which requires only one dose. The latter has not yet been distributed in the country.

Table (2) below represent the cumulative number of administered and received doses for each vaccines until the end of July.

Vaccines used	administered doses	received doses	Efficiency rate
Pfizer	1555606	1718514	95%
AstraZeneca/Oxford	240193	580760	70%
Sputnik V	44753	119986	91.60%
CoronaVac	332219	699994	50.38%
Johnson and Johnson	0	0	66%

TABLE 1 – DISTRIBUTION OF VACCINES IN TUNISIA

Vaccines used	administered doses	Efficiency rate
Pfizer	81 490 504	95%
AstraZeneca/Oxford	7 838 931	70%
Moderna	12 357533	50.38%
Johnson and Johnson	1 074 197	66%

TABLE 2 – DISTRIBUTION OF VACCINES IN France

The first dose of COVID-19 vaccine in France was received for the first time in December 27, 2020. Since that, the number of doses has multiplied rapidly to protect the population as quickly as possible. On the other side of the Mediterranean, Tunisia started vaccinating its population in March 13, 2021. the vaccination campaign was slow given the country's economic situation. the number of administrated doses increased in July, 2021. Figure 2 illustrate the daily number of vaccinations administrated in Tunisia and France.

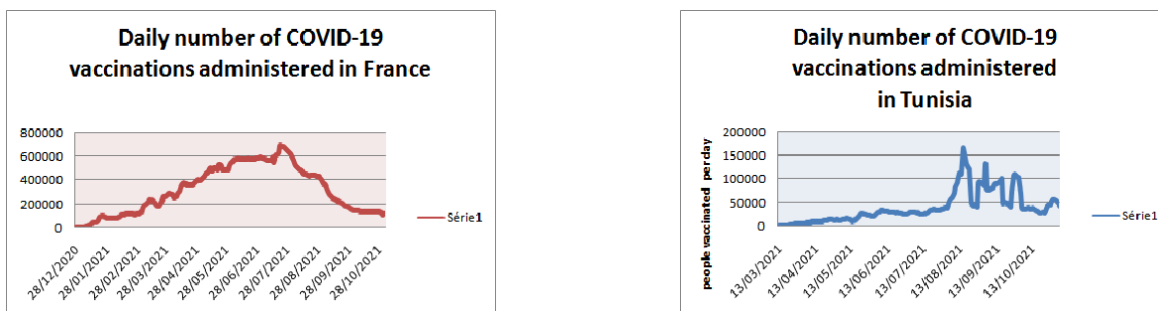


FIGURE 2 – Daily number of Covid-19 vaccinations administered in France and Tunisia

4.1 SEAIR model before vaccination

In this section, we perform some numerical simulations for the previous model to provide estimates for the evolution of the COVID-19 outbreak in France and Tunisia. We present simulation results by solving the Constrained Optimal Control Problem Applied to Vaccination. In the numerical simulations, we compare the optimal intervention strategies under different settings of proportion of infections, waiting rate to viral shedding, symptom onset and the infection rate

among vaccines. The values of model parameters were obtained by the best available local data and literature reviews of previous studies [8,14]. Table 1 provides a summary of the definitions and values of the parameters.

For simplicity and straightforward analysis of causality, we take initial conditions

$$\begin{aligned}
 S_0 &= N_0 - I_0 \\
 (26) \quad E(0) &= A(0) = R(0) = VS(0) = VE(0) = VA(0) = VI(0) = VP(0) = VR(0) = 0 \\
 D(0) &= 0.
 \end{aligned}$$

First, we consider the model (1) before the vaccine deployment, that is $\psi = 0$, during the period from December, 2020 through October, 2021. We assume that the vaccinated subpopulations VP , VS , VE and VI are equal to zero. The set of differential equations was solved using Matlab.

In this part, we focus on some numerical results for SEAIR model before vaccination in France and Tunisia. Figure 3 presents the ODEs simulation of the SEAIR model (1) for France before vaccination (the case $\psi = 0$).

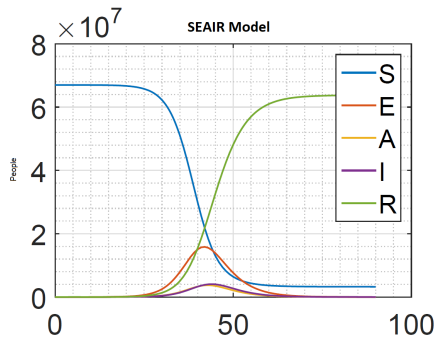


FIGURE 3 – the model solutions before the vaccination programm in France

The allure of the SEAIR model in Tunisia is the same like France case but in two different period. By vaccine effect we can see that The Tunisian case is translated.

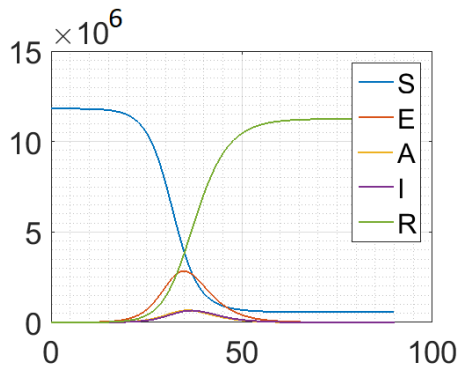


FIGURE 4 – SEAIR model for Tunisia case

4.2 Vaccination effect In Tunisia and France

In France, these results is given for the period from February 15, 2021 to April 30, 2021 when the number of cases go past 50000 infected cases (Figure 5). Vaccination is highly concentrated.

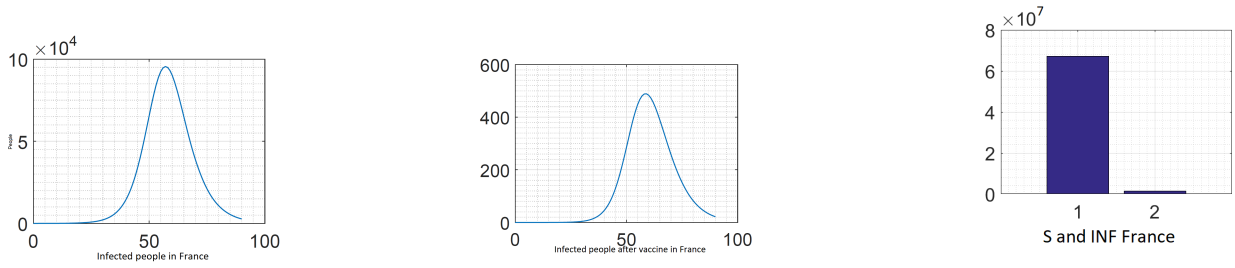


FIGURE 5 – Comparaison infected people in France before and after vaccination

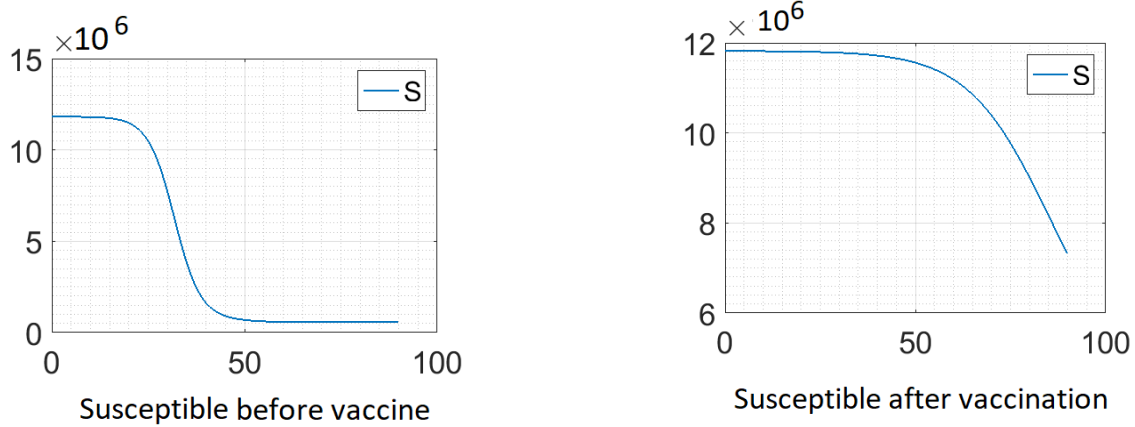


FIGURE 6 – Comparaison between Susceptible people in Tunisia before and after vaccination

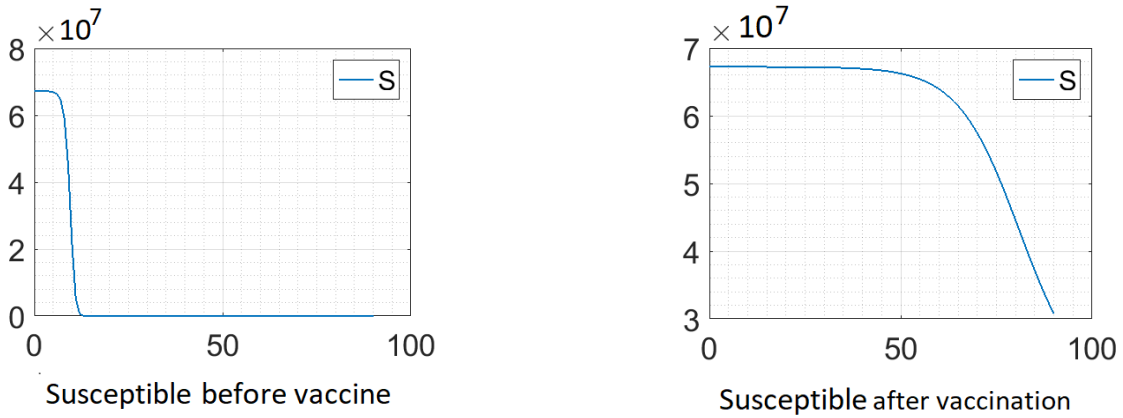


FIGURE 7 – Comparaison between Susceptible people in France before and after vaccination

From Figure 7, we can observe that the convergence of Susceptible people after vaccination converge slowly which return to the increasing number of vaccinated people, barrier protection and the number of infected people in the first wave. Under the optimal vaccination, Infected people are gradually decreasing in time. The right part of Figure 5 proves by the increasing of the person vaccinated the amplitude of the infected person goes to 500. The decreasing of the number of infected people influence to the number of death in the same period (Figure 8).

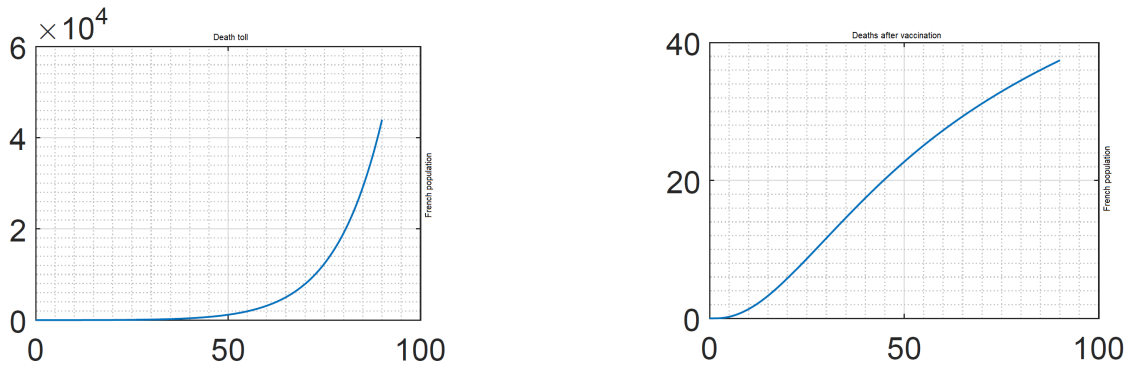


FIGURE 8 – Comparaison death people in France before and after vaccination

For the case of Tunisia, the strongest wave is in the period between May 15, 2021 and July 15, 2021 which returns to the "delta various" of COVID-19. The influence of that is the big number of death which was 20000. the strategy of vaccination in Tunisia is so late if we compare it with case of France.

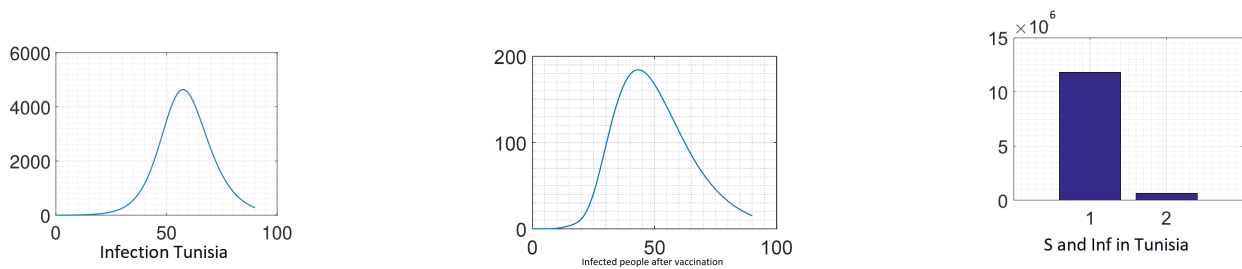


FIGURE 9 – Comparaison infected people in Tunisia before and after vaccination

4.3 THIRD WAVE :OMICRON

we consider the model (1) before the vaccine deployment, that is $\psi = 0$, during the period from December, 2021 through March, 2022.

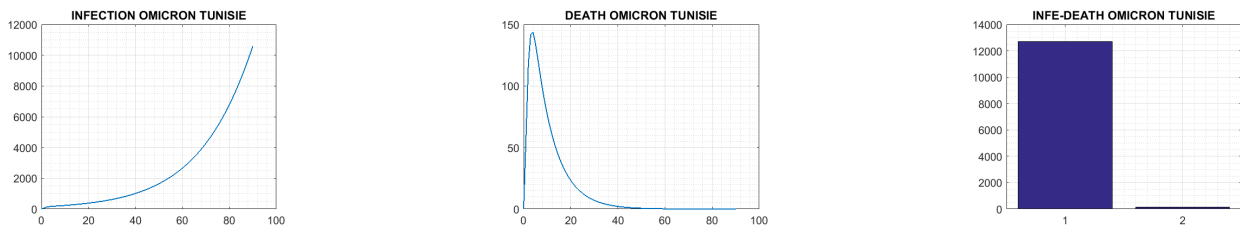


FIGURE 10 – Comparaison infected people and death in Tunisia

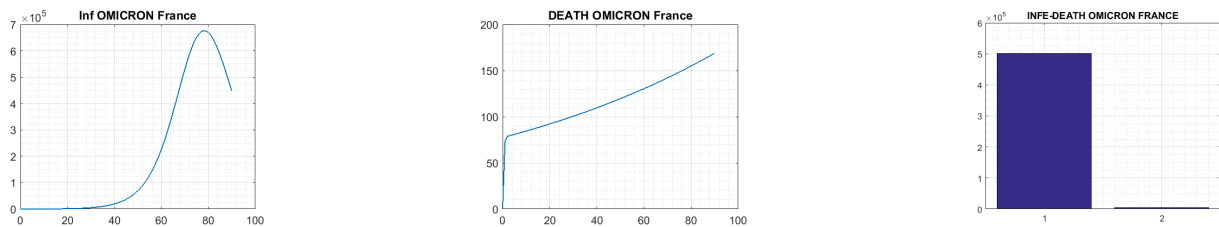


FIGURE 11 – Comparaison between infected people and death in France

From Figures 10 and 11, we can see that the number of Infected people increase very quickly with exponential behavior (characteristic of Omicron various) but the number of death is too small, if we compare with the two previous waves. We can remark that also by the histogram which describe the difference between the maximum of death and infected people in this period.

5 Conclusion

Firstly, by using an optimal control theory, we show that, assuming a quadratic cost for the control effort at a given time ($c(t)$), an optimal control strategy significantly reduces the number of deaths and is particularly sustainable at the population level.

Secondly, we performed a numerical simulation on our model using repository data on the outbreak of COVID-19 in France and Tunisia to estimate the effect of the vaccination strategies. By comparing the two countries, we remark that, in France, the vaccination is highly concentrated in the early stage of epidemic for early possible strategy and the vaccinated proportion stays constant. In Tunisia, the strategy of vaccination was started in August, that why the benefit of vaccination is significantly reduced as the time of the start of vaccination from pandemic onset is delayed.

Time-dependent vaccination is computed and analysed using SEAIR model. Vaccination is among the most important control measures for reducing the spread of many infectious diseases. Thus, it is of great interest to develop an efficient time schedule and prioritization of limited vaccine supplies. This study uses a mathematical model of the transmission dynamics and employs techniques from control theory to derive optimal intervention strategies.

Finally, accelerating the application of vaccines, combined with maintaining a low transmission rate by following preventive measures would result in an even better strategy for curtailing the pandemic and reducing the number of deaths.

Références

- [1] **L. Cesari.** *Optimization Theory and Applications : Problems with Ordinary Differential Equations.* Springer-Verlag, New York, (1983).
- [2] **J. Danane, K. Allali, Z. Hammouch, K. S. Nisar.** *Mathematical analysis and simulation of a stochastic COVID-19 Levy jump model with isolation strategy.* Results in Physics, 23-103994, Elsevier (2021).
- [3] **R. Djidjou Demasse, Y. Michalakis, M. Choisy, M. T. Sofonea, S. Alizon.** *Optimal COVID-19 epidemic control until vaccine deployment.* medRxiv. Cold Spring Harbor Laboratory Press (2020).
- [4] **H. Gaff, E. Schaefer.** *Optimal control applied to vaccination and treatment strategies for various epidemiological models* MATHEMATICAL BIOSCIENCES AND ENGINEERING, Volume 6, Number 3, (2009).
- [5] **I.M. Hezam, A. Foul, A. Alrasheedi.** *A dynamic optimal control model for COVID-19 and cholera co-infection in Yemen.* Advances in Difference Equations, 2021 :108, SpringerOpen Journal (2021).

- [6] **D.M. Himmelblau.** *Applied Nonlinear Programming* , McGraw-Hill, New York, (1972).
- [7] **J. Kim, H.D. Kwon, J. Lee.** *Constrained optimal control applied to vaccination for influenza.* Computers and Mathematics with Applications V. 71, Issue 11, pp. 2313-2329 (2016).
- [8] **F. Lin, , K. Muthuraman, M. Lawley.** *An optimal control theory approach to non-pharmaceutical interventions.* BMC Infect Dis 10(1) :32. (2010).
- [9] **A.G.C. Perez, D.A. Oluyori.** *An extended SEIARD model for COVID-19 vaccination in Mexico : analysis and forecast.* Mathematics in Applied Sciences and Engineering doi : 10.5206-14233 (2021).
- [10] **T. A. Perkins, G. Espana.** *Optimal Control of the COVID-19 Pandemic with Non-pharmaceutical Interventions.* Bulletin of Mathematical Biology 82 :118, Society for Mathematical Biology (2020).
- [11] **L.S. Pontryagin, V.G. Boltyanskii, R.V. Gamkrelidze, E.F. Mishchenko.** *The Mathematical Theory of Optimal Processes* Vol. 528, Interscience Publishers John Wiley and Sons, Inc., New York-London, p. 28. (1962)
- [12] **J. A. Snyman, C. FP.Angos AND Y. Yavin** *Penalty function solutions to optimal control problems with general constraints via a dynamic optimasition method,* Computers Math. Applic. Vol. 23, No. 11, pp. 47-55, (1992).
- [13] **A. Tesfay, T. Saeed, A. Zeb, D. Tesfay, A. Khalaf, J. Brannan.** *Dynamics of a stochastic COVID-19 epidemic model with jump-diffusion.* Advances in Difference Equations, 2021 :228, SringerOpen journal (2021).